

Tactile Man–Robot Interaction for an Industrial Service Robot

Steen Kristensen¹, Mathias Neumann², Sven Horstmann¹, Frieder Lohnert¹,
and Andreas Stopp¹

¹ DaimlerChrysler Research and Technology, Cognition and Robotics Group
Alt-Moabit 96A, D-10559 Berlin, Germany
{steen.kristensen, sven.horstmann, frieder.lohnert,
andreas.stopp}@daimlerchrysler.com

² Technische Universität Berlin
Institut für Technische Informatik
Franklinstraße 28/29
D-10587 Berlin, Germany
mathiasn@cs.tu-berlin.de

Abstract. In this paper, research towards a cooperative robotic assistant for manufacturing environments is presented. The aim of this research is to develop a robotic assistant which can easily be instructed how to either perform tasks autonomously or in cooperation with humans. Focus of this paper is on the tactile interaction between man and robot which is used for teaching as well as for direct cooperation in tasks jointly performed by worker and robot.

1 Introduction

In this paper we describe past and ongoing research efforts at DaimlerChrysler Research and Technology’s Cognition and Robotics Group where over the last years work has been conducted on human-friendly robots for space, office, and factory automation.

A major goal of this work has been (and still is) to develop robots that can assist, co-exist with, and be taught by humans. Therefore, apart from developing the “standard” mobile robot capabilities such as landmark recognition, path planning, obstacle avoidance etc. our research effort has been aimed at the development of learning capabilities that will allow the user to quickly and intuitively teach the robot new environments, new objects, new skills, and new tasks. We believe this is the only viable way of creating robotic assistants that can be flexible enough to function robustly in the very diverse habitats of humans and thus be accepted as truly helpful devices. In this paper we present some of the results of this work.

Current research is aimed towards improving the man-machine interaction by adding more advanced communication and cognition capabilities. This has the purpose of further simplifying the teaching of the robot but also to make it more “cooperative” by having it interpret human commands and behaviour in the

given context, allowing it to make better decisions about when, how, and where to assist the human co-worker(s). An important criterion is, however, that the robot can also perform tasks autonomously once instructed/taught by a human worker. Additionally it should be able to learn incrementally, i.e. to improve its performance during task execution by “passively” receiving or actively requesting information (the latter could for example be in the case where the robot detects ambiguities which it cannot autonomously resolve).

A typical scenario for a new robotic assistant in an industrial setting would be:

- The robot is led through the factory halls and is shown important places (stores, work stations, work cells etc.),
- the robot is shown relevant objects, e.g. tools, work pieces, and containers,
- the robot is shown how to dock by work cells, containers etc. in order to perform the relevant manipulation tasks,
- the robot is taught how to grasp various objects and how (and possibly in what sequence) to place them in corresponding containers or work cells,
- in case of a cooperation task, the robot is shown when and how to assist the human worker.

For service robots in manufacturing it is important that the man–robot communication channels are robust and unambiguous rather than high bandwidth (in the information theoretic sense). The need for high robustness is motivated by the fact that mistakes/misinterpretations on the side of the robot can have severe consequences economically as well as for the safety of the human workers. On the other hand are the environments typically more ordered and the range of tasks more restricted as is the case for domestic service robots. This means that robustness can partly be achieved through using a set of low bandwidth channels. Tactile sensing using a force/torque sensor is an example of such a channel with which a limited amount of information can robustly be conveyed to the robot.

In Section 2 some more background in terms of related work and project specific constraints are outlined. In Sections 3–6 various methods for interaction and cooperation based on force/torque sensing are presented. Finally in Section 7, the results are discussed and summarised.

2 Background

In previous work [1], we have described how we can interactively teach new environments in a quick and robust manner. The environment models are represented as topological graphs [2, 3] well-known from various mobile robot applications [4–7]. The topological graphs we use are extended with metric and symbolic information about objects such as work stations and places such as rooms or stores. An example of a model is shown in Figure 1.

In general, the world model can be said to contain elements which are relatively static over longer time spans. This has the obvious advantage that the

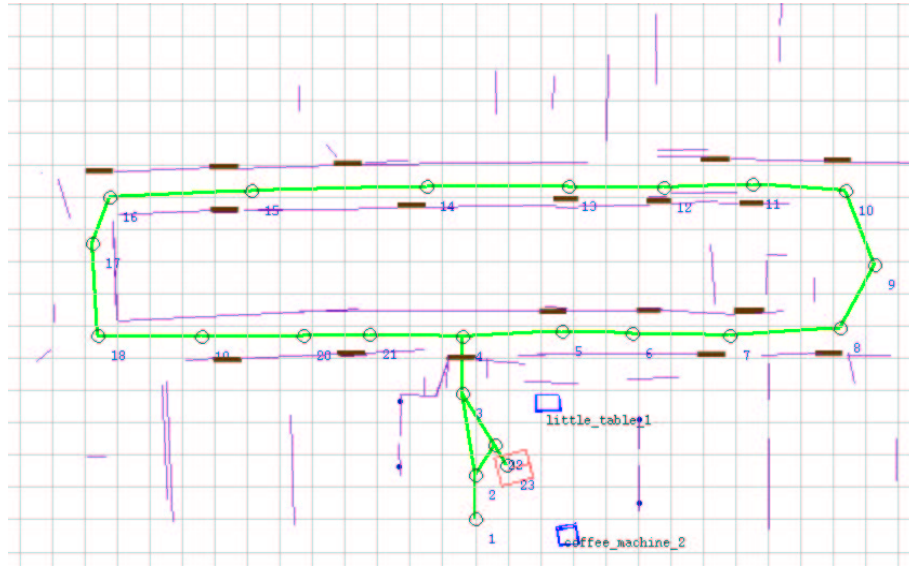


Fig. 1. World model taught by leading the robot through a previously unvisited office environment. Grid size is 1 meter. The thick lines and the circles they are connecting is the basic topological graph. The thin lines are the walls, the black bars are the doors. The squares represent special objects, such as work stations, which are modelled in 3D.

model only needs to be occasionally updated. Furthermore, the symbolic nature of the model means that it forms a good basis for planning of high level missions like “fetch object A in store room 12”. However, this kind of model does not form a sufficient basis for planning and executing detailed manipulation and cooperation tasks. For this purpose we have developed a number of sensor-based skills which allows the user to interact with the robot for controlling the posture of the robot, for handing over objects, and for interactively teaching the robot how to grasp and manipulate objects.

The robot, Clever, we use for the development of various interaction schemes is shown in Figure 2. Clever can be seen as a technology demonstrator which serves as the basis for later “real” industrial service robots which will be able to carry and manipulate heavier loads.

On Clever, a force/torque sensor is mounted in the wrist of the manipulator, i.e. between the arm and the gripper. This has the advantage that the same sensor can be used for sensor based cooperation, manipulation and for compliant motion, where the user “takes the robot by the hand” which we have found to be an intuitive and straightforward way for humans to interact with the robot.

The drawback of using only one sensor is that the force/torque measurement system cannot distinguish between the user induced forces and torques and those resulting from the payload of the manipulator. In service robots for domestic use where the payloads are typically light (mass < 1kg) the user may well be able



Fig. 2. The robot “Clever” used in the experiments. The robot consists of a differential drive platform equipped with a 7-DOF Amtec manipulator and a Sick lidar plus a set of colour CCD cameras mounted on a pan/tilt unit. The arm is equipped with a force/torque sensor between the wrist and the gripper, which is a standard parallel jaw gripper with force sensors in the “fingers”.

to compensate for the load of the work piece when guiding the robot using compliant motion. For an industrial service robot, potentially carrying significantly heavier weights, this is not an option, though. Therefore it is necessary for the robot to be able to distinguish between user and payload induced forces and torques. How we do this is outlined in Section 3.

The mobile manipulator as a whole has nine degrees of freedom. Therefore the problem of redundancy has to be solved, i.e. a method is needed to determine the posture of the mobile manipulator. Often mobile manipulators are modelled as one kinematic chain. But the used nonholonomic mobile platform has a slower response to movement commands than the manipulator. We expect this to be characteristic of all industrial service robots which will tend to have heavy platforms which it is not possible nor sensible to control at high command rates. In Section 4 an approach to force guidance is presented which takes the different character of both subsystems into account [8].

The special problem of force guidance is that the direction of the movement is actually controlled by the operator without the robot knowing what the actual purpose of the movement is. This means that the trajectories cannot be attuned to the task. Therefore the control algorithm as described in Section 4 tends to result in the platform following the tool in a quite sub-optimal manner.

Situations where the platform gets in the way of itself are possible. In particular, the used nonholonomic platform makes it difficult to change the position to one parallel to the forward direction of the robot, causing for example shunting to be quite time-consuming.

In order to solve this problem in a pragmatic way, the raw force/torque signal from the FTS is surveyed. The operator should be enabled to control both: tool location and posture of the mobile manipulator. An approach to implement a system for this purpose is presented in Section 4.5.

3 Calibration of the Force/Torque Measurement System

As argued above, it is necessary to be able to on-line (re-)calibrate the force/torque measurement system to account for any payload held in the gripper when moving the manipulator using compliant motion.

If the robot carries a (rigid) workpiece the payload induced force/torques are nearly constant¹ for a fixed orientation of the TCP. However, when the orientation of the TCP is changed as a result of a user guiding the arm using compliant motion, the forces and torques caused by the gripper and the payload change. To compensate for those effects it is necessary to know the mass and the vector to the center of gravity (relative to the FTS) of the combined gripper/payload object. Having such a model, it is possible to calculate the forces and torques induced by the gripper/payload for any given TCP orientation and thus to determine the forces and torques applied externally to the manipulator.

how do we calibrate.....??

This approach has been shown to work well for slow movements (where centrifugal forces can be ignored) like force guidance initiated by humans.

4 Coordination of the Manipulator and the Mobile Platform

Clever's manipulator can change its position freely as desired in the range limited by its working space. Due to this and to the slower and kinematically more constraint performance of the platform it appears reasonable that the force/torque guided motion is performed mainly relative to the platform by moving the tool center point (TCP).

4.1 Force/Torque Guided Motion of the Manipulator

Usual force guidance is implemented in the way that the velocity of the tool is a linear function of forces $\mathbf{F}(t) = (F_x(t), F_y(t), F_z(t))^T$ and torques $\mathbf{M}(t) = (M_x(t), M_y(t), M_z(t))^T$ [9].

However, the used manipulator arm cannot be controlled by velocities. Instead the goal configuration and a time interval that results from the control

¹ If the platform moves with accelerations which are small compared to gravity.

rate f_c are used to control the arm in position mode. Furthermore the noisy sensor signal requires filtering to ensure that only reasonable large signals are taken into account.

The following non-linear function is proposed:

$${}^P\mathbf{r}\left(t + \frac{1}{f_c}\right) = {}^P\mathbf{r}(t) + \frac{{}^Pv_{\max}}{f_c} \begin{pmatrix} \text{sign}(F_x(t)) e^{(1 - \frac{F_{\max}}{|F_x(t)|})} \\ \text{sign}(F_y(t)) e^{(1 - \frac{F_{\max}}{|F_y(t)|})} \\ \text{sign}(F_z(t)) e^{(1 - \frac{F_{\max}}{|F_z(t)|})} \end{pmatrix} \quad (1)$$

The desired position ${}^P\mathbf{r}$ of the tool at time $t + \frac{1}{f_c}$ is reached from the current position at time t in compliance with $0 < |F_{x,y,z}(t)| \leq F_{\max}$. ${}^Pv_{\max}$ specifies the maximal permitted translation velocity of the tool with respect to the platform frame.

The desired orientation ${}^P\mathbf{A}_R$ at time $t + \frac{1}{f_c}$ can be described by:

$${}^P\mathbf{A}_R\left(t + \frac{1}{f_c}\right) = \mathbf{R}_{XYZ}(w_x, w_y, w_z) {}^P\mathbf{A}_R(t) \quad (2)$$

Where \mathbf{R}_{XYZ} is a matrix representing the rotations of the TCP around the axes of the platform frame. The three rotation angles are defined as:

$$w_{x,y,z} = \frac{{}^P\omega_{\max}}{f_c} \text{sign}(M_{x,y,z}(t)) e^{(1 - \frac{M_{\max}}{|M_{x,y,z}(t)|})} \quad (3)$$

$0 < |M_{x,y,z}(t)| \leq M_{\max}$ has to hold and ${}^P\omega_{\max}$ specifies the maximal permitted rotation velocity of the tool with respect to the platform frame.

4.2 Compensation of Platform Movements

The platform as the second subsystem is able to move simultaneously and independently. But the tool should only be moved with respect to the fixed world frame according to the forces applied to the FTS. Therefore the manipulator has to compensate the movements of the platform.

Let ${}^W\mathbf{p}(t) = ({}^Wp_x(t), {}^Wp_y(t), {}^Wp_\phi(t))^T$ denote the position (a reference point in the center, Figure 3) and the orientation of the platform with respect to the world frame. ${}^W\mathbf{p}(t)$ is known from the platform's odometry sensing.

The transformation

$${}^Wp_x\left(t - \frac{1}{f_c}\right) + {}^P r_x(t) \cos({}^Wp_\phi\left(t - \frac{1}{f_c}\right)) - {}^P r_y(t) \sin({}^Wp_\phi\left(t - \frac{1}{f_c}\right)) = {}^Wp_x(t) + ({}^P r_x(t) + {}^P \Delta r_x) \cos({}^Wp_\phi(t)) - ({}^P r_y(t) + {}^P \Delta r_y) \sin({}^Wp_\phi(t)) \quad (4)$$

$${}^Wp_y\left(t - \frac{1}{f_c}\right) + {}^P r_x(t) \sin({}^Wp_\phi\left(t - \frac{1}{f_c}\right)) + {}^P r_y(t) \cos({}^Wp_\phi\left(t - \frac{1}{f_c}\right)) = {}^Wp_y(t) + ({}^P r_x(t) + {}^P \Delta r_x) \sin({}^Wp_\phi(t)) + ({}^P r_y(t) + {}^P \Delta r_y) \cos({}^Wp_\phi(t)) \quad (5)$$

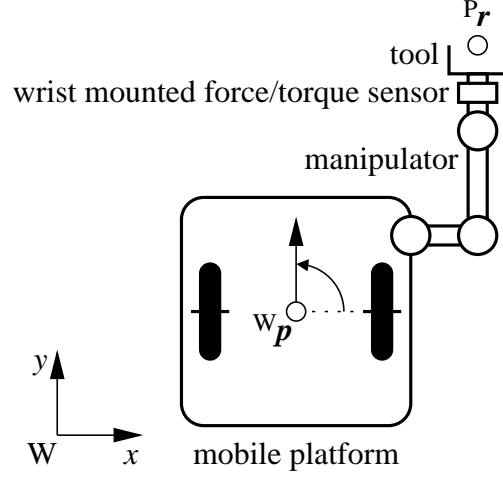


Fig. 3. The mobile manipulator and its reference points. ${}^W\mathbf{p}$ is the reference point of the platform between the wheels (black areas) and ${}^P\mathbf{r}$ is the reference point of the arm at the end of the tool (TCP). Orientation is given by the angle about the x-axis of the fixed world frame and the driving direction (arrow).

of the current x-y-coordinates of the tool with respect to the platform into the world frame on the basis of the current and the last configuration of the platform results in the offsets

$$\begin{aligned}
{}^P\Delta r_x &= -{}^P r_x(t) \\
&+ {}^P r_x(t) \cos({}^W p_\phi(t) - {}^W p_\phi(t - \frac{1}{f_c})) \\
&+ {}^P r_y(t) \sin({}^W p_\phi(t) - {}^W p_\phi(t - \frac{1}{f_c})) \\
&+ (-{}^W p_x(t) + {}^W p_x(t - \frac{1}{f_c})) \cos({}^W p_\phi(t)) \\
&+ (-{}^W p_y(t) + {}^W p_y(t - \frac{1}{f_c})) \sin({}^W p_\phi(t))
\end{aligned} \tag{6}$$

$$\begin{aligned}
{}^P\Delta r_y &= -{}^P r_y(t) \\
&- {}^P r_x(t) \sin({}^W p_\phi(t) - {}^W p_\phi(t - \frac{1}{f_c})) \\
&+ {}^P r_y(t) \cos({}^W p_\phi(t) - {}^W p_\phi(t - \frac{1}{f_c})) \\
&+ ({}^W p_x(t) - {}^W p_x(t - \frac{1}{f_c})) \sin({}^W p_\phi(t)) \\
&+ (-{}^W p_y(t) + {}^W p_y(t - \frac{1}{f_c})) \cos({}^W p_\phi(t))
\end{aligned} \tag{7}$$

for moving in the x-y-plane and

$$\Delta w_z = {}^W p_\phi(t) - {}^W p_\phi(t - \frac{1}{f_c}) \quad (8)$$

for rotating around the z-axis of the world. These offsets have to be added in equations 1 and 2.

4.3 Preferred Configurations of the Manipulator

Based on the computed target position ${}^P \mathbf{r}(t + \frac{1}{f_c})$ and the associated configuration it is possible to determine a preferred configuration close to ${}^P \mathbf{r}(t + \frac{1}{f_c})$ which provides more manipulability [10]. To reach this configuration the mobility of the platform should be used without moving the tool with respect to the world frame.

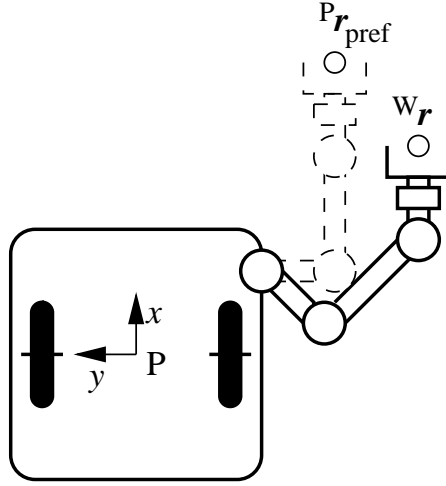


Fig. 4. The preferred point ${}^P \mathbf{r}_{\text{pref}}$ is fixed relatively to the platform. The platform has to move to match ${}^P \mathbf{r}_{\text{pref}}$ with ${}^W \mathbf{r}$.

The mobile platform is able to move only in the x-y-plane of the world which is parallel to the x-y-plane of the platform frame. Therefore a new position of the tool

$$\begin{pmatrix} {}^P r_{\text{pref},x}(t + \frac{1}{f_c}) \\ {}^P r_{\text{pref},y}(t + \frac{1}{f_c}) \end{pmatrix} \quad (9)$$

can be found with respect to the platform which yields a more favourable configuration of the manipulator (Figure 4). The z-coordinate and the orientation in the world frame must be constant.

4.4 Closed Loop Platform Controller

The only task of the platform is to move in the next interval so that the arm will be able to take on its preferred configuration [11].

The used nonholonomic mobile platform has the following decoupling matrix Φ which describes the correlation between the velocities of the preferred point in work space and in configuration space.

$$\Phi(\mathbf{p}(t)) = \begin{pmatrix} \Phi_{11}(\mathbf{p}(t)) & \Phi_{12}(\mathbf{p}(t)) \\ \Phi_{21}(\mathbf{p}(t)) & \Phi_{22}(\mathbf{p}(t)) \end{pmatrix} \quad (10)$$

$$\begin{aligned} \Phi_{11}(\mathbf{p}(t)) &= \cos(\mathbf{p}_\phi(t)) \\ \Phi_{12}(\mathbf{p}(t)) &= -{}^P r_{\text{pref},x}(t + \frac{1}{f_c}) \sin(\mathbf{p}_\phi(t)) - {}^P r_{\text{pref},y}(t + \frac{1}{f_c}) \cos(\mathbf{p}_\phi(t)) \\ \Phi_{21}(\mathbf{p}(t)) &= \sin(\mathbf{p}_\phi(t)) \\ \Phi_{22}(\mathbf{p}(t)) &= {}^P r_{\text{pref},x}(t + \frac{1}{f_c}) \cos(\mathbf{p}_\phi(t)) - {}^P r_{\text{pref},y}(t + \frac{1}{f_c}) \sin(\mathbf{p}_\phi(t)) \end{aligned} \quad (11)$$

With the transformation

$$\begin{aligned} {}^W r_{\text{pref},x}(t + \frac{1}{f_c}) &= {}^W p_x(t) \\ &\quad + {}^P r_{\text{pref},x}(t + \frac{1}{f_c}) \cos(\mathbf{p}_\phi(t)) \\ &\quad - {}^P r_{\text{pref},y}(t + \frac{1}{f_c}) \sin(\mathbf{p}_\phi(t)) \\ {}^W r_{\text{pref},y}(t + \frac{1}{f_c}) &= {}^W p_y(t) \\ &\quad + {}^P r_{\text{pref},x}(t + \frac{1}{f_c}) \sin(\mathbf{p}_\phi(t)) \\ &\quad + {}^P r_{\text{pref},y}(t + \frac{1}{f_c}) \cos(\mathbf{p}_\phi(t)) \end{aligned} \quad (12)$$

and the gain g_P the control vector

$$\begin{pmatrix} v_{\text{lin}} \\ v_{\text{rot}} \end{pmatrix} = \Phi^{-1}(\mathbf{p}(t)) \mathbf{v} \quad (13)$$

with

$$\mathbf{v} = \begin{pmatrix} {}^W \dot{r}_x + g_P \left({}^W r_x(t + \frac{1}{f_c}) - {}^W r_{\text{pref},x}(t + \frac{1}{f_c}) \right) \\ {}^W \dot{r}_y + g_P \left({}^W r_y(t + \frac{1}{f_c}) - {}^W r_{\text{pref},y}(t + \frac{1}{f_c}) \right) \end{pmatrix} \quad (14)$$

can be computed considering the desired velocity of the tool.

In the next step the arm has to compensate this movement as mentioned above.

4.5 Controlling the Posture According to the User's Intention

The solution of the redundancy problem depends on the desired task which is determined by the operator. Therefore the user's intention has to be predicted.

The following situation might occur: The tool is at the desired location in the world. However, the platform has the wrong orientation (not to the purpose of the user's intention). It should move sideways to turn around the tool.

Corresponding forces and torques can be applied by the user but the machine moves only the tool because of the force guidance algorithm as mentioned above. The user's intention is not regarded.

Inspired by the way humans are moving large objects on a surface with friction the following approach has been developed.

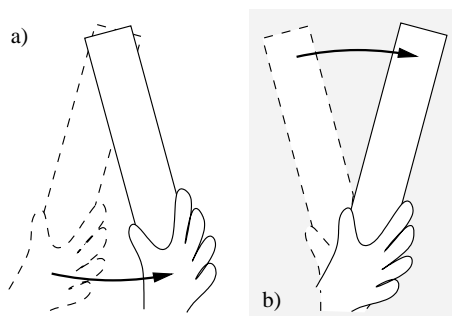


Fig. 5. Two possible cases to move large objects with one hand on a frictional surface.

Consider the bar in Figure 5. In the case of turning it around the grasp point (Figures 5b and 6b) the ratio of the force and the torque is easily to be distinguished from that of the rotation about the opposite point (Figures 5a and 6a).

If the bar is representing the mobile manipulator, then the movement, as shown at Figure 5a, is equivalent to the known mode of force guidance. In case of Figure 5b a new mode is defined leading to sideways movements.

It is quite obvious from Figure 6 that only F_y and M_z are important for moving sideways. The ratio of both signals decides on the desired mode of motion.

Figure 7 shows the regions which can be characterized as modes of moving. The gray shaded regions correspond to the cases 6b and 6d and will lead to changes of the posture. Selecting the ranges it has to be ensured that displacement along the y-axis (dashed ellipse) and orientation change of the tool around the z-axis (scored ellipse) remain possible. The modes shown in Figure 6a and 6c have to be allowed too. These regions of pairs of (F_y, M_z) are called force/torque symbols of modes of movement.

The expression

$$\kappa = \frac{-\arctan(\varrho(F_y(t)M_z(t) - \varepsilon))}{\pi} + \frac{1}{2} \quad (15)$$

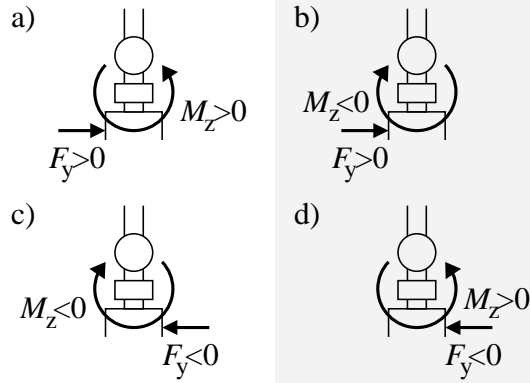


Fig. 6. Possibilities to apply significant values of force and torque to the tool.

determines the membership of a measured pair of (F_y, M_z) to the gray shaded regions of Figure 7. ϱ specifies the smoothness and ε specifies the threshold of the regions. The values for ϱ and ε have been determined empirically.

4.6 Moving the Virtual Preferred Point

As described above, forces and torques induced by the operator may be interpreted as intention to move sideways (gray shaded regions in Figure 7). But performing sideways movements imply complicated manoeuvres because of the nonholonomic constraints. A sufficiently fast reaction of the platform is not feasible.

Rather, the force component is used to gain experience with this way of operation, in order to overlay the preferred point (9) with a supplementary offset ${}^P\Delta r_{\text{pref},y}$. This offset is computed iteratively by

$${}^P\Delta r_{\text{pref},y}(t + \frac{1}{f_c}) = {}^P\Delta r_{\text{pref},y}(t) + \kappa h \text{sign}(F_y(t)) e^{(1 - \frac{F_{\text{max}}}{|F_y(t)|})} \quad (16)$$

That does in itself not change the position of the platform but the changed orientation enables another shunting behaviour.

The relation of force, moment and velocity of the preferred point displacement is quite complex and can thus be difficult to handle by the operator. Therefore the factor h has to be carefully determined which we have done experimentally.

The offset ${}^P\Delta r_{\text{pref},y}$ has to be integrated in the platform controller as described in Section 4.4. The force guided movement of the tool (Section 4.1) has to be scaled by $1 - \kappa$ respectively.

Of course, this method makes it impossible for the system to change the orientation and position of the tool independently and freely. But mostly such movements can be emulated in two steps.

Which steps?.....

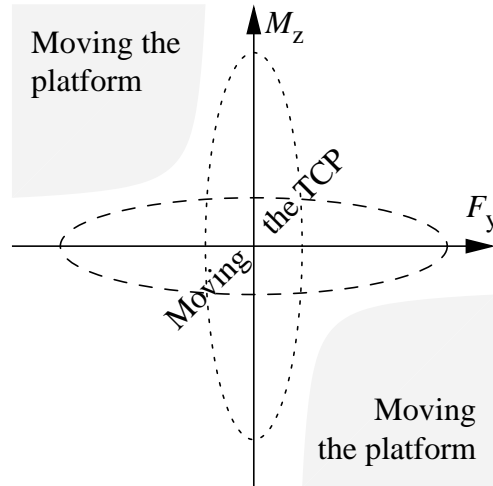


Fig. 7. Regions of force-moments pairs (F_y, M_z) . Each area represents a simple mode of moving.

4.7 Experiments

A good example to show the advantages of the proposed method is to try to achieve a sideways displacement by moving on a zigzag course. This manoeuvre is expected to be used frequently when humans cooperate with robotic assistants.

For the experiments, the system shown in Figure 2 was used.

A simplified control architecture, as shown in Figure 8, was used. Due to the communication structure and driver software the control rate is limited to 4Hz.

To demonstrate the functionality, the mobility of the arm was limited to that of the platform (x-y-plane). ${}^W\dot{\mathbf{r}}$ was set to 0 and g_P was set to 1 because slow motion was tried first. ρ was set to 1 and ε to $-50\text{N}^2\text{m}$ (determined experimentally).

Figure 9 and Figure 10 show roughly the same movement of the platform. The starting points are equivalent to the situation shown in Figure 3. In the second case the operator had the possibility to displace the preferred point. It can be seen that in order to achieve a greater sideways displacement of the platform, a smaller movement of the tool is required.

5 Teaching of Arm Movements

For teaching the arm movements necessary to perform manipulation tasks we have pursued two directions; teaching via a graphical user interface and teaching by directly moving the arm around using compliant motion. Normally, the “crude” movements are taught using the GUI while finer movements are better taught by directly moving the arm to the desired position and orientation.

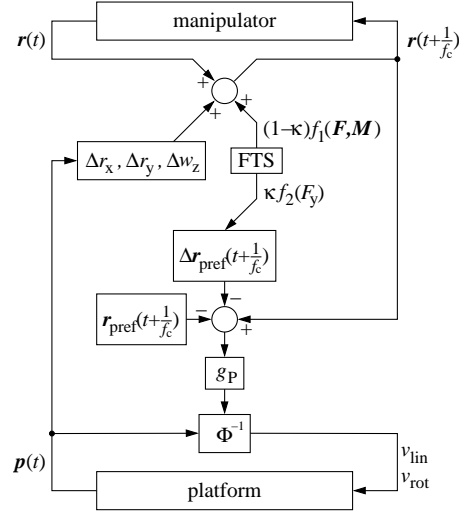


Fig. 8. Simplified block diagram of the controller. Both (platform and arm) controllers and the relations between them are shown.

In order to be able to generalise grasping and manipulation movements to cases, where the objects and/or positions to place them are different from when they were taught, the movements are recorded relative to the objects and not relative to the robot's frame of reference. This means that initially the object of interest has to be located with respect to the robot.

For the recognition and localisation of objects not easily describable with geometric primitives we use the *iterative closest point* (ICP) algorithm [12]. This has the advantage that object models can be generated simply by scanning the object with a laser range finder and cutting out the relevant part of the resulting 3D point cloud. The algorithm iteratively seeks to match model points to scene points (using a nearest neighbour metric) and—based on this match—to register the model and the scene objects. When the iteration has converged we compare the mean square error between scene and model points, and if this is below a given threshold, we assume the scene object to be of the same type as the model object and that these furthermore coincide. Due to its simplicity, the algorithm works rather quickly, but due to the fact that it is basically a gradient descent, it has problems with local minima. However, for scenes where foreground and background can easily be segmented, it has been shown to work well. In Figure 11 an example of the localisation of a workpiece on a table is shown.

Knowing the pose of the object relative to the robot, it is straightforward to transform and store the arm movements performed by the user in a teaching “run” in object centered coordinates. Thus, when the robot operates autonomously, it can transform the taught trajectories according to the given current pose of the object and so perform the manipulation at this new, relative

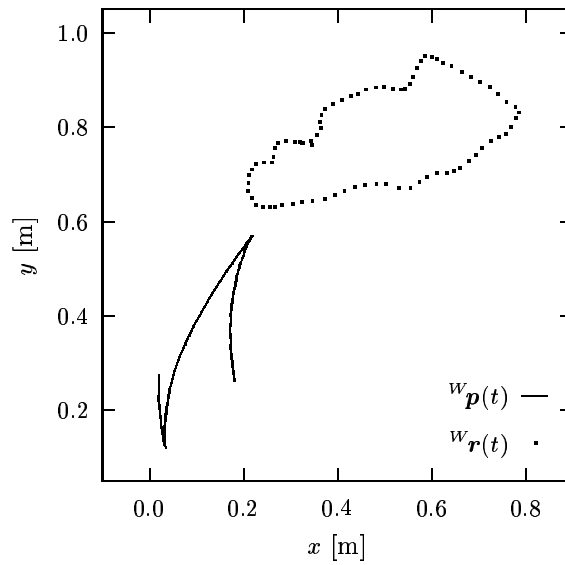


Fig. 9. Positions of the platform (${}^W\mathbf{p}(t)$) and the tool (${}^W\mathbf{r}(t)$) when moving without changing the preferred point (classical force guided motion).

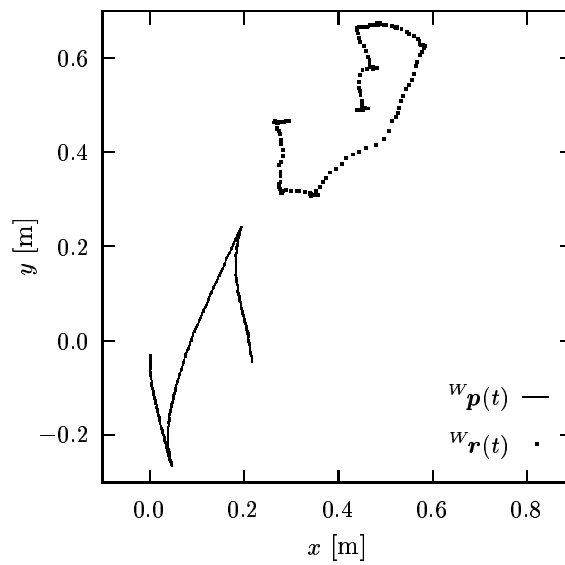


Fig. 10. Positions of the platform and the tool by shunting the robot with the special meaning of the force/torque signal.

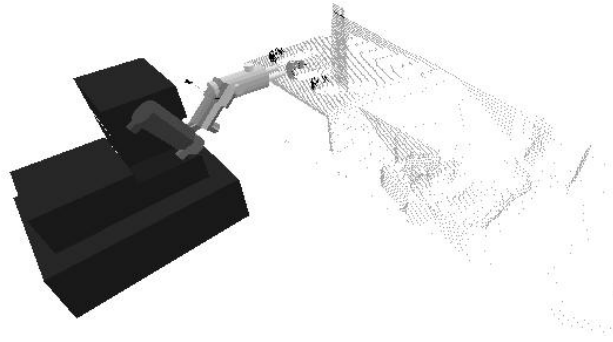


Fig. 11. Example of the localisation of an object on a table. The scene consisting of a table with 3 cups on it (see Figure ?? for an image of a similar scene) has been scanned by the robot’s laser range finder resulting in the 3D point cloud in the right half of the image. The ICP algorithm has converged to the cup in the middle (the lighter model points cover the darker scene points). On the basis of this localisation it is calculated how to grasp the cup which is shown in the display as feedback to the user.

position. We have demonstrated the validity of this method with various tasks such as picking up workpieces and placing them into workstations.

We are currently investigating how to generalise taught grasping trajectories to different classes of objects. Also we are developing methods for interactively extending and improving already existing trajectories.

6 Handing Over Objects

Finally, we would like to present an example of a simple skill showing how tactile sensing combined with acoustic feedback (i.e. two low bandwidth channels) can be combined to achieve a very useful and robust functionality for man–robot interaction.

The straightest and simplest way of man–robot cooperation is to deliver a workpiece to a worker by the robot. That means that the manipulator presents the load so that it can be easily taken by a human if the gripper of the manipulator is releasing it. For domestic applications with light objects, an object can simply be released when the user signals that he/she has taken hold of it (f.ex. using speech input or by shaking the object a little). The problem in an industrial context, where objects up to a weight of 10 kg can be handled, is that the human cannot sense the weight of the object until it is released by the robot. If the object is heavier than expected, this may lead to the human dropping it, possibly causing injury.

To ensure that such accidents are avoided, we have implemented a skill that makes the robot release the object only when the user already supports its full weight. Knowing the weight of the gripper and the object from calibration this is easy to measure using the force/torque sensor. As feedback to the user, signalling

if he/she has to lift more or less, a tone is produced which height increases until a certain level at which two short tone pulses are generated, indicating that the user is now supporting the full weight of the object. The robot then waits a short period, and if the weight is still supported by the user, the gripper is opened.

Albeit extremely simple (or maybe exactly because of that), this skill has proven to be intuitively easy to understand and thus very useful in our cooperation experiments.

7 Discussion and Conclusion

In this paper, we have described research done for a service robot for manufacturing at DaimlerChrysler Research and Technology.

In particular, we presented methods developed for tactile interaction for cooperation and for teaching the robot manipulation skills and trajectories using a single wrist mounted force/torque sensor.

First we outlined how we on-line calibrate the payload of the manipulator which enables the user to teach and cooperate using compliant motion even when the robot is carrying a heavy object in its gripper.

Second we presented results from current research on extending “classical” methods for coordinated arm/platform movements with methods for the estimation of the user’s intentions. Knowing these intentions will allow the robot to better determine how to move as a result of the forces and torques induced by the user, thus making the cooperation faster, less straining, and more intuitive for the user. First results from shunting experiments were presented. However, more work is required on how to define preferred configurations and how to select one if several exist. Furthermore we will investigate to what extent force/torque “symbols” can be used to initiate manoeuvres possibly in combination with other communication channels such as speech and vision.

Then we outlined how we teach various manipulation trajectories in a sensoric context, allowing for generalisation to cases where objects’ poses and/or the positions to place those vary.

Finally, as an example of a simple but very efficient and robust cooperation skill, we presented a method using acoustic feedback to ensure that the worker is not surprised and thus injured by the weight of a workpiece when this is handed over by the robot.

We would like to emphasize the fact that the presented methods are developed in the context of a larger system which is used as a research platform for human–robot interaction in the manufacturing process. This provides us with a unique opportunity to test and evaluate these techniques together with other learning and interaction methods (based on speech, vision, and laser sensors). The lesson we have learned so far is—maybe not surprisingly—that a combination of simple, robust and partly redundant interaction mechanisms leads to a safer and faster to learn interaction than do more sophisticated methods based on a single sensor. Therefore we will continue to explore such systems since safety

and ease of use (which also has a positive effect on safety) are of paramount importance in manufacturing where on the other hand the cost of adding another sensor is not as critical as for robots aimed at the mass consumer market.

Acknowledgements

This research was partly sponsored by the German Ministry for Education and Research under the projects NEUROS, Neural Skills for Intelligent Robot Systems, and MORPHA, Intelligent Anthropomorphic Assistance Systems.

References

1. Kristensen, S., Hansen, V., Horstmann, S., Klandt, J., Kondak, K., Lohnert, F., Stopp, A.: Interactive Learning of World Model Information for a Service Robot. In: *Sensor Based Intelligent Robots. Lecture Notes in Artificial Intelligence (1724)*, Springer (1999) 49–67
2. Kuipers, B.J., Buyn, Y-T.: A Robust, Qualitative Method for Robot Spatial Learning. In: *Proceedings of the Seventh National Conference on Artificial Intelligence*. AAAI Press, Menlo Park, Calif. (1988) 774–779
3. Kuipers, B.J., Buyn, Y-T.: A Robot Exploration and Mapping Strategy Based on a Semantic Hierarchy of Spatial Representations. *Robotics and Autonomous Systems*, Vol. 8 (1991), 47–63
4. Gutmann, J-S., Nebel, B.: Navigation mobiler Roboter mit Laserscans. In: *Autonome Mobile Systeme*. Springer (1997), in German.
5. Koenig, S., Simmons, R.G.: Xavier: A Robot Navigation Architecture Based on Partially Observable Markov Decision Process Models. In: Kortenkamp, D., Bonasso, R.P., Murphy, R.: *Artificial Intelligence and Mobile Robots*. AAAI Press/The MIT Press (1998) 91–122
6. Thrun, S., Bücken, A., Burgard, W., Fox, D., Fröhlinghaus, T., Hennig, D., Hofmann, T., Krell, M., Schmidt, T.: Map Learning and High-Speed Navigation in RHINO. In: Kortenkamp, D., Bonasso, R.P., Murphy, R.: *Artificial Intelligence and Mobile Robots*. AAAI Press/The MIT Press (1998) 21–52
7. Jensfelt, P., Kristensen, S.: Active Global Localisation for a Mobile Robot Using Multiple Hypothesis Tracking. In: *Workshop on Reasoning with Uncertainty in Robot Navigation (Workshop ROB-3 at the International Joint Conference on Artificial Intelligence)*, Stockholm, Sweden (1999) 13–22
8. Chung, J.H., Velinsky, S.A., Hess, R.A.: Interaction Control of a Redundant Mobile Manipulator. *The International Journal of Robotics Research*, Vol. 17(12) (1998) 1302–1309
9. Kazanzides, P., Zuhars, J., Mittelstadt, B., Taylor, R.H.: Force Sensing and Control for a Surgical Robot. In: *Proceedings of the 1992 IEEE International Conference on Robotics and Automation (1992)* 612–617
10. Yoshikawa, T.: *Foundations of Robotics: Analysis and Control*. The MIT Press, Cambridge, Massachusetts (1990)
11. Yamamoto, Y.: *Control and Coordination of Locomotion and Manipulation of a Wheeled Mobile Manipulator*. Ph.D.-Thesis, Department of Computer and Information Science School of Engineering and Applied Science, University of Pennsylvania (1994)

12. Besl, P.J., McKay, N.D.: A Method for Registration of 3-D Shapes. *IEEE Transactions on Pattern Analysis and Machine Intelligence*, Vol. 14(2) (1992) 239–256